

# Self-similar inverse cascade from generalized symmetries

Yuji Hirono,<sup>1,\*</sup> Kohei Kamada,<sup>2,3,4,†</sup> Naoki Yamamoto,<sup>5,‡</sup> and Ryo Yokokura<sup>6,§</sup>

<sup>1</sup>*Department of Physics, Osaka University, Toyonaka, Osaka 560-0043, Japan*

<sup>2</sup>*School of Fundamental Physics and Mathematical Sciences, Hangzhou Institute for Advanced Study, University of Chinese Academy of Sciences (HIAS-UCAS), 310024 Hangzhou, China*

<sup>3</sup>*International Centre for Theoretical Physics Asia-Pacific (ICTP-AP), Hangzhou/Beijing, China*

<sup>4</sup>*Research Center for the Early Universe, The University of Tokyo, Bunkyo-ku, Tokyo 113-0033, Japan*

<sup>5</sup>*Department of Physics, Keio University, Yokohama 223-8522, Japan*

<sup>6</sup>*Department of Physics & Research and Education Center for Natural Sciences, Keio University, Yokohama 223-8521, Japan*

(Dated: January 15, 2025)

We investigate the role of generalized symmetries in driving non-equilibrium and non-linear phenomena, specifically focusing on turbulent systems. While conventional turbulence studies have revealed inverse cascades driven by conserved quantities integrated over the entire space, such as helicity in three spatial dimensions, the influence of higher-form symmetries, whose conserved charges are defined by integration over subspaces, remains largely unexplored. We demonstrate a novel mechanism where higher-form symmetries naturally induce a self-similar inverse cascade. Taking axion electrodynamics with non-linear topological interaction as a paradigmatic example, we show that the conserved charge associated with its 1-form symmetry drives the system toward large-scale coherent structures through a universal scaling behavior characterized by analytically determined scaling exponents. Our findings suggest that higher-form symmetries can provide a fundamental organizing principle for understanding non-equilibrium phenomena and the emergence of coherent structures in turbulent systems.

*Introduction.*—Generalized symmetries [1] have emerged as a powerful framework for understanding the fundamental structure of physical theories, extending beyond the conventional point-particle symmetries to include higher-form symmetries acting on extended objects such as loops or surfaces. These symmetries have provided crucial insights into quantum field theories including gauge theories [2–5] and condensed matter systems [6]. Their spontaneous breaking patterns and associated dynamics have been particularly important in understanding the organizing principles of various physical systems [1, 7–12].

Despite the considerable attention these symmetries have received in vacuum (or equilibrium) physics, their role in non-equilibrium phenomena remains relatively unexplored. This gap in our understanding is particularly notable given the ubiquity of non-equilibrium processes in nature and their significance in various physical systems, from condensed matter physics, plasma physics, and astrophysics to cosmology.

In this Letter, we report a novel connection between higher-form symmetries and turbulent behavior, specifically focusing on the emergence of inverse cascade phenomena [13–16]. While inverse cascades have been well established in systems with conserved charges defined by integration over the entire space domain, such as energy and enstrophy in two-dimensional turbulence [13, 14] or helicity in three-dimensional flows [17, 18], we demonstrate that higher-form symmetries, whose conserved charges are defined by integration over subspaces, can naturally induce a self-similar inverse cascade, where energy or conserved quantities flow hierarchically from small to large scales. We exemplify this mechanism for

axion electrodynamics with the non-linear topological interaction, which possesses a 1-form symmetry and associated conservation law [19–23]. Our argument can also be applied to other systems with higher-form symmetries considered in, e.g., Ref. [24]. This suggests a new paradigm for understanding the emergence of coherent structures in turbulent systems from fundamental properties of higher-form symmetries, with potential implications across a broad range of physical scenarios.

*Higher-form symmetry and instability in axion electrodynamics.*—As a demonstration of our mechanism, we consider an example of the axion electrodynamics with a massless axion and a gauge field in  $(3 + 1)$ -dimensions. The action is given by

$$S = \int d^4x \left( -\frac{v^2}{2} \partial_\mu \phi \partial^\mu \phi - \frac{1}{4e^2} f_{\mu\nu} f^{\mu\nu} - \frac{C}{4} \phi f_{\mu\nu} \tilde{f}^{\mu\nu} \right), \quad (1)$$

where  $\phi$  is a dimensionless pseudo-scalar field identified as an axion,  $f_{\mu\nu} = \partial_\mu a_\nu - \partial_\nu a_\mu$  is the field strength of a  $U(1)$  gauge field  $a_\mu$ ,  $v$  is a parameter with mass dimension 1,  $e$  is a coupling constant, and  $C = 1/(4\pi^2)$ . The symbol  $\tilde{f}^{\mu\nu} = \frac{1}{2} \epsilon^{\mu\nu\rho\sigma} f_{\rho\sigma}$  with the totally anti-symmetric tensor  $\epsilon^{\mu\nu\rho\sigma}$  denotes the dual of the field strength. The equations of motion of this system read

$$\begin{aligned} v^2 \partial_\mu \partial^\mu \phi - \frac{C}{4} f_{\mu\nu} \tilde{f}^{\mu\nu} &= 0, \\ \frac{1}{e^2} \partial_\mu f^{\mu\nu} + C(\partial_\mu \phi) \tilde{f}^{\mu\nu} &= 0. \end{aligned} \quad (2)$$

The system has been shown to exhibit instability in the presence of background electric fields [24–27]. Under a uniform nonzero electric field  $f_{03}(0, \mathbf{x}) = -\bar{E}_3$ , the dispersion relation for modes with momentum  $\mathbf{k} = (k_1, 0, 0)$

takes the form

$$\omega^2 = k_1^2 \pm \frac{Ce\bar{E}_3}{v}|k_1|. \quad (3)$$

This reveals an unstable mode in the infrared region  $0 < |k_1| < Ce\bar{E}_3/v$ .

Through the conservation laws, we can demonstrate that this instability necessarily reduces the electric field. The conserved charges associated with the 0-form symmetry  $\phi \rightarrow \phi + \lambda$  and 1-form symmetry  $a_\mu \rightarrow a_\mu + \lambda_\mu$  are

$$\begin{aligned} Q_\phi(\mathcal{V}) &= K_\phi(\mathcal{V}) + T_\phi(\mathcal{V}), \\ Q_a(\mathcal{S}) &= K_a(\mathcal{S}) + T_a(\mathcal{S}), \end{aligned} \quad (4)$$

respectively, where we have defined

$$K_\phi(\mathcal{V}) = \int_{\mathcal{V}} d\tilde{V}_\mu v^2 \partial^\mu \phi, \quad T_\phi(\mathcal{V}) = - \int_{\mathcal{V}} d\tilde{V}_\mu \frac{C}{4} a_\nu \tilde{f}^{\mu\nu}, \quad (5)$$

$$K_a(\mathcal{S}) = \frac{1}{2} \int_{\mathcal{S}} dS^{\mu\nu} \frac{1}{e^2} \tilde{f}_{\mu\nu}, \quad T_a(\mathcal{S}) = -\frac{1}{2} \int_{\mathcal{S}} dS^{\mu\nu} C \phi f_{\mu\nu}. \quad (6)$$

with  $\mathcal{V}$  and  $\mathcal{S}$  being 3- and 2-dimensional closed subspaces. We have decomposed the conserved charges into those from the kinetic terms,  $K_\phi(\mathcal{V})$  and  $K_a(\mathcal{S})$ , and those from the topological terms,  $T_\phi(\mathcal{V})$  and  $T_a(\mathcal{S})$ .<sup>1</sup>

While  $Q_\phi$  is the total helicity consisting of the chiral charge  $K_\phi$  carried by axions and the usual magnetic helicity  $T_\phi$ ,  $Q_a$  is a conserved charge associated with the 1-form symmetry consisting of the electric flux  $K_a$  and the topological charge  $T_a$ . The charge  $T_a$  has a geometric meaning of the linking number, similar to the usual magnetic helicity [24]. By taking  $\mathcal{S}$  as an  $x^1x^2$ -plane with  $x^3 = 0$  at the time  $x^0$  denoted by  $S_{12}(x^0)$ , we have

$$Q_a(S_{12}(x^0)) = - \int_{S_{12}(x^0)} dS^{12} \left( \frac{1}{e^2} f_{03} + C \phi f_{12} \right). \quad (7)$$

At initial time  $x^0 = 0$ , the surface integral is dominated by  $K_a(S_{12}(0))$  with the initial electric field  $f_{03} = -\bar{E}_3$ . Meanwhile, the tachyonic growth of  $\phi$  and  $f_{12}$  generates the topological charge  $T_a(S_{12}(x^0))$ . Consequently, the conservation law dictates that  $K_a(S_{12}(x^0))$  and electric field  $f_{03}$  decrease.

<sup>1</sup> Note that  $T_\phi(\mathcal{V})$  and  $T_a(\mathcal{S})$  are not invariant under large gauge transformations. They can be made invariant under those transformations by rewriting them in terms of the topological quantum field theories (TQFT), and the resulting symmetries become non-invertible [22–24, 28, 29]. However, as we will not consider the backgrounds with 't Hooft lines or axionic vortices, this reformulation will not matter in the following discussion, and we will write these topological quantities without introducing TQFT.

To understand the physical nature of this mechanism, it is instructive to compare it with the chiral plasma instability (CPI) that occurs in the presence of fermion chirality imbalance [30, 31]. In the CPI, the generation of magnetic helicity leads to a reduction of the initial chirality imbalance due to total helicity conservation. In our case, the role of helicity conservation is replaced by the conservation law associated with the 1-form symmetry, suggesting this can be viewed as a generalized chiral instability [24].

*Dissipation.*—In realistic situations in a medium, we must account for dissipative effects. As a concrete setup, we consider a system coupled to gapped charged matter, where the Ohmic current is absent. However, the axion field can still experience dissipation through its interactions with environmental degrees of freedom. By integrating out these modes,<sup>2</sup> we obtain the following equation of motion for the axion:

$$v^2(-\partial_0^2 + \nabla^2)\phi - \gamma\partial_0\phi - \frac{C}{4}f_{\mu\nu}\tilde{f}^{\mu\nu} = 0, \quad (8)$$

where  $\gamma$  is the diffusion coefficient. Importantly, the presence of  $\gamma$  preserves both the unstable mode and the conservation law (7). This preservation of the conservation law in the presence of dissipation sets the stage for a novel cascade mechanism.

*Mechanism of inverse cascade.*—The interplay between dissipation and charge conservation provides a fundamental mechanism for the inverse cascade. The dissipation term  $\gamma\partial_0\phi$  reduces the total energy of the system over time. However, the conserved charge  $Q_a = K_a + T_a$  must remain constant due to the 1-form symmetry. Initially,  $Q_a$  is dominated by the kinetic component  $K_a$  from the electric field. As the instability develops, this charge is transferred to the topological component  $T_a$ , which eventually dominates the late-time dynamics. Since the charge density at wavenumber  $\sim k$  contributes energy  $\sim k^2$  through spatial derivatives, maintaining constant charge while minimizing energy necessarily drives the system toward smaller  $k$  modes. This mechanism continuously transfers the topological charge to larger scales.

Our numerical simulation confirms this inverse cascade mechanism. Additionally, we observe the emergence of self-similar scaling behavior, where energy and topological charge are hierarchically transferred to increasingly larger scales. As we demonstrate through scaling analysis below, this leads to universal scaling exponents  $\alpha = 1, \beta = 1/2$  characterizing the late-time evolution of the system.

*Set up for numerical simulations.*—To demonstrate the emergence of self-similar inverse cascade, we numerically

<sup>2</sup> This procedure can be done systematically at the level of the action using the formulation of Refs. [32, 33].

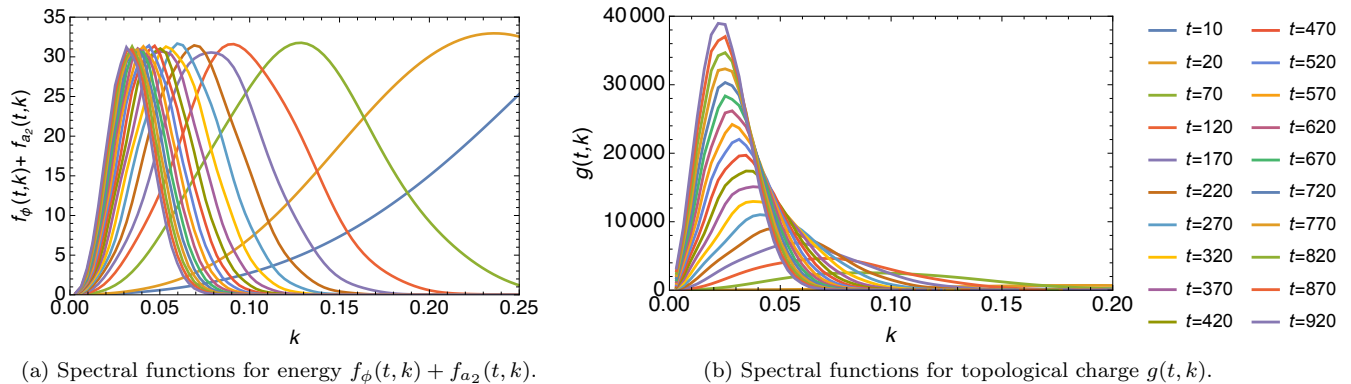


FIG. 1: Spectral functions for energy and topological charge at different times. Both spectral functions exhibit the inverse cascade.

analyze the long-time behavior of the system. While the full  $(3 + 1)$ -dimensional dynamics involves complex interplay between all field components, the essential mechanism of generalized symmetry-induced cascade can be captured by studying field variations along a single direction.<sup>3</sup> Specifically, we assume the system is homogeneous along the  $x^2$ - and  $x^3$ -directions, and the field  $a_3$  is spatially homogeneous,  $a_3(x^\mu) = a_3(x^0)$ . Under these conditions and in the temporal gauge  $a_0 = 0$ , the equations of motion reduce to

$$v^2(-\partial_0^2\phi + \partial_1^2\phi) - \gamma\partial_0\phi = -C\partial_0a_3\partial_1a_2, \quad (9)$$

$$\partial_0f^{01} = 0, \quad (10)$$

$$\frac{1}{e^2}(-\partial_0^2a_2 + \partial_1^2a_2) = C\partial_1\phi\partial_0a_3, \quad (11)$$

$$-\frac{1}{e^2}\partial_0^2a_3 = C(\partial_0\phi\partial_1a_2 - \partial_1\phi\partial_0a_2). \quad (12)$$

We solve the system in a box,  $x^1 \in [-L, L]$ , with the periodic boundary condition. First, we focus on the conservation law obtained by Eq. (12). The conserved charge integrated along the  $x^1$ -direction can be written as

$$N = \int_{-L}^L dx^1 \left( \frac{1}{e^2}\partial_0a_3 + C\phi\partial_1a_2 \right) = \frac{2Lv}{Ce^3}A(x^0) + N_{\text{top}}, \quad (13)$$

where

$$A(x^0) := \frac{Ce}{v}\partial_0a_3(x^0) \quad (14)$$

is proportional to the spatial average of the electric field,

$$N_{\text{top}} := C \int_{-L}^L dx^1 \phi\partial_1a_2 \quad (15)$$

<sup>3</sup> A similar approximation is employed in the analysis of the CPI in the presence of magnetic fields [34].

is the topological charge, and  $Q_a(S_{12}(x^0)) = \int dx^2 N$ . The quantity  $A(x^0)$  determines the scale below which the modes exhibit instability as in Eq. (3).

To simplify our notation, we introduce the coordinates  $(t, x) := (x^0, x^1)$ , dimensionless fields  $(b, c) := (e^2\phi, ea_2/v)$ , and the rescaled parameter  $\sigma := \gamma/v^2$ . The equations of motion for  $b$  and  $c$  then take the form

$$\partial_t^2 \begin{pmatrix} b \\ c \end{pmatrix} + \sigma\partial_t \begin{pmatrix} b \\ 0 \end{pmatrix} = \begin{pmatrix} \partial_x^2 & A\partial_x \\ -A\partial_x & \partial_x^2 \end{pmatrix} \begin{pmatrix} b \\ c \end{pmatrix}. \quad (16)$$

To solve Eq. (16) in momentum space, we expand  $b(t, x)$  and  $c(t, x)$  as

$$b(t, x) = \frac{b_e(t, k_0)}{2} + \sum_{n=1}^{\infty} (b_e(t, k_n) \cos k_n x + b_o(t, k_n) \sin k_n x),$$

$$c(t, x) = \frac{c_e(t, k_0)}{2} + \sum_{n=1}^{\infty} (c_e(t, k_n) \cos k_n x + c_o(t, k_n) \sin k_n x),$$

where discrete momenta are given by  $k_n = \pi n/L$ .

*Numerical results.*—We numerically solve Eq. (16) in momentum space for  $\{b_{e,o}(t, k_n), c_{e,o}(t, k_n)\}_{n=1, \dots, N_k}$ , where  $N_k$  sets the UV cutoff. Our analysis uses the parameters  $L = 1000$ ,  $N_k = 200$ ,  $\sigma = 1.0$ ,  $e = 1.0$ , and  $v = 1$ , with initial conditions  $N = 24\pi^2 L$  and  $(b_{e,o}(0, k_n), c_{e,o}(0, k_n)) = (0, 2, 0, 0)$  for  $n = 1, \dots, N_k$ . The initial value  $A(0)$  is given by  $A(0) = Ce^3 N/(2L) \simeq 3.0$ .

We now analyze the time evolution of physical quantities. The energy of the  $\phi$  and  $a_2$  fields and the topological charge can be expressed using the Fourier coefficients  $\{b_{e,o}(t, k_n), c_{e,o}(t, k_n)\}_{n=1, \dots}$  as

$$E_X = \frac{v^2 L}{2e^2} \sum_{n=1}^{\infty} f_X(t, k_n), \quad X = \phi, a_2, \quad (17)$$

$$N_{\text{top}} = \frac{CLv}{e^3} \sum_{n=1}^{\infty} k_n g(t, k_n), \quad (18)$$

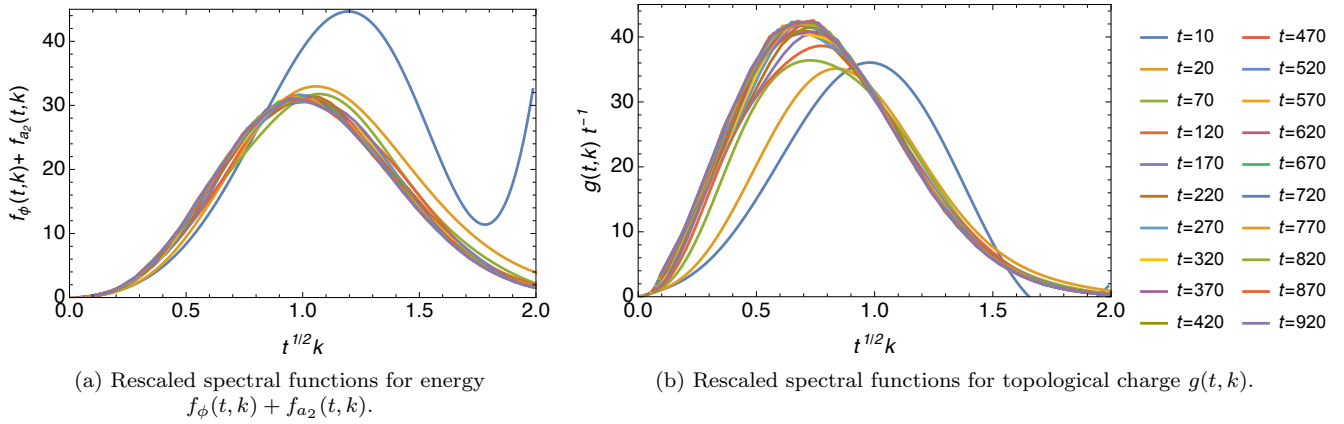


FIG. 2: Rescaled spectral functions for energy and topological charge at different times according to the scaling laws (26)–(28). Both rescaled spectral functions converge at later times, indicating self-similarity.

where we introduced spectral functions by

$$f_\phi(t, k_n) := \sum_{i=e,o} [(\partial_t b_i(t, k_n))^2 + k_n^2 (b_i(t, k_n))^2], \quad (19)$$

$$f_{a_2}(t, k_n) := \sum_{i=e,o} [(\partial_t c_i(t, k_n))^2 + k_n^2 (c_i(t, k_n))^2], \quad (20)$$

$$g(t, k_n) := b_e(t, k_n) c_o(t, k_n) - b_o(t, k_n) c_e(t, k_n). \quad (21)$$

In Fig. 1, we plot the spectral functions  $f_\phi(t, k) + f_{a_2}(t, k)$  and  $g(t, k)$  of the energy and topological charge, respectively, at different times. The results show that the  $a_2$  and  $\phi$  fields, initially amplified by the generalized chiral instability, develop inverse cascades at later times.

*Self-similar scaling induced by higher-form symmetries.*—The late-time dynamics of the system exhibits self-similar behavior, which we characterize through scaling analysis. We propose that the Fourier components take the scaling form

$$b_i(t, k) \sim t^{\alpha/2} \tilde{b}_i(t^\beta k), \quad c_i(t, k) \sim t^{\alpha/2} \tilde{c}_i(t^\beta k), \quad (22)$$

for  $i = e, o$ . The exponents  $\alpha$  and  $\beta$  can be determined from the equations of motion and conservation laws, as we show below. The scaling ansatz (22) implies that the spectral function  $g(t, k)$  obeys

$$g(t, k) \sim t^\alpha \tilde{g}(t^\beta k). \quad (23)$$

To find  $\beta$ , we examine the structure of Eq. (16). In the late-time regime, the first-order time derivative term becomes dominant in Eq. (16). The  $(\partial_x)^2$  term generates time dependence of the form  $tk^2 = (t^{1/2}k)^2$  upon integration, requiring  $\beta = 1/2$ . For consistency, the  $A\partial_x$  term, which contributes  $k \int^t A(t') dt'$  must also scale as  $t^{1/2}k$ . This consistency condition determines the scaling of  $A(t)$ :

$$A(t) \sim t^{-1/2}. \quad (24)$$

The decay of  $A(t)$  indicates that the conserved charge  $N$  becomes dominated by its topological component  $N_{\text{top}}$  at late times. In the scaling regime, this topological charge takes the form

$$\int dk k g(t, k) = t^{\alpha-2\beta} \int dy \tilde{g}(y), \quad (25)$$

where  $y := t^\beta k$ . The constancy of this quantity requires  $\alpha = 2\beta$ , yielding our final scaling exponents:

$$\alpha = 1, \quad \beta = \frac{1}{2}. \quad (26)$$

These scaling exponents lead to the following relations for the spectral functions:

$$f_\phi(t, k) \sim \sum_{i=e,o} (k b_i(t, k))^2 \sim y^2 \tilde{f}_\phi(y) \quad (27)$$

and analogous scaling for  $f_{a_2}(t, k)$ , and

$$g(t, k) \sim t \tilde{g}(y). \quad (28)$$

Note that the kinetic energies in  $f_\phi(t, k)$  and  $f_{a_2}(t, k)$  scale as  $\propto t^{-1}$  and become subdominant.

These theoretical predictions are confirmed by our numerical simulations. Figure 2(b) shows the spectral function rescaled according to Eq. (26), demonstrating clear convergence to a universal curve at late times. Figure 3 shows the time evolution of the charges stored in  $N_{\text{kin}}$  and  $N_{\text{top}}$  as well as the inverse of the coherence length  $\xi$  defined by

$$\xi := \frac{\sum_n k_n^{-1} (f_\phi(t, k_n) + f_{a_2}(t, k_n))}{\sum_n (f_\phi(t, k_n) + f_{a_2}(t, k_n))}. \quad (29)$$

Both  $N_{\text{kin}}$  (or equivalently,  $A(t)$ ) and  $\xi^{-1}$  show asymptotic behavior  $t^{-1/2}$ , consistent with the predicted scaling (24), further validating our scaling analysis. It should be emphasized that this self-similar inverse cascade is due

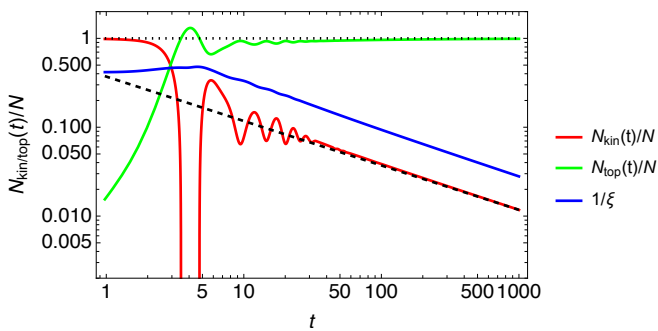


FIG. 3: Time evolution of  $N_{\text{kin}}$  (red),  $N_{\text{top}}$  (green), and  $\xi^{-1}$  (blue). Black dashed line illustrates  $t^{-1/2}$  asymptotic behavior of  $N_{\text{kin}}$  and  $\xi^{-1}$ .

to the conservation law (7) associated with the 1-form symmetry and the transfer of the charge from the initial electric field to the topological charge.

*Summary and discussion.*—In this Letter, we have demonstrated that higher-form symmetries can induce self-similar inverse cascade in a turbulent system. Using axion electrodynamics as a concrete example, we showed that starting from an initial electric field configuration that triggers the generalized chiral instability, the system exhibits characteristic scaling behavior at late times. Specifically, the spectral function  $g(t, k)$  obeys the scaling law  $g(lt, k) \sim lg(t, l^{1/2}k)$ , while the instability parameter  $A(t)$  decays as  $t^{-1/2}$ .

Interestingly, these scaling exponents match those of turbulence after the CPI [34–38], suggesting a broader universality class encompassing systems with higher-form symmetries. This universality suggests similar phenomena may emerge in other systems with higher-form symmetries across diverse physical scenarios, from condensed matter to cosmology. The turbulent behavior we describe could be experimentally tested in magnetic materials where magnetic fluctuations serve as emergent axion fields [26]. Similar dynamics may also manifest in gauge field amplification during inflation [39, 40] in the presence of spectator axion-like fields.

Our analysis can be extended to the full  $(3 + 1)$ -dimensional axion electrodynamics to uncover additional features of the cascade process. Furthermore, exploring connections between our findings and other non-equilibrium systems with higher-form symmetries may reveal new universal aspects of turbulent behavior.

*Acknowledgments.*—This work was supported in part by JSPS KAKENHI Grant Numbers JP22H05111 (Y.H.), JP22H05111 (Y.H.), JP22H05118 (Y.H.), JP24K23186 (Y.H.), JP23K17687 (K.K.), JP22H01216 (N.Y.), JP24K00631 (N.Y.), JP21K13928 (R.Y.), JST, PRESTO Grant Number JPMJPR24K8 (Y.H.), and the National Natural Science Foundation of China (NSFC) under Grant Number 12347103 (K.K.).

\* yuji.hirono@gmail.com

† kohei.kamada@ucas.ac.cn

‡ nyama@rk.phys.keio.ac.jp

§ ryokokur@keio.jp

- [1] D. Gaiotto, A. Kapustin, N. Seiberg, and B. Willett, *JHEP* **02**, 172 (2015), arXiv:1412.5148 [hep-th].
- [2] P. R. S. Gomes, *SciPost Phys. Lect. Notes* **74**, 1 (2023), arXiv:2303.01817 [hep-th].
- [3] S. Schafer-Nameki, *Phys. Rept.* **1063**, 1 (2024), arXiv:2305.18296 [hep-th].
- [4] T. D. Brennan and S. Hong, (2023), arXiv:2306.00912 [hep-ph].
- [5] L. Bhardwaj, L. E. Bottini, L. Fraser-Taliente, L. Gladdeen, D. S. W. Gould, A. Platschorre, and H. Tillim, *Phys. Rept.* **1051**, 1 (2024), arXiv:2307.07547 [hep-th].
- [6] J. McGreevy, *Ann. Rev. Condensed Matter Phys.* **14**, 57 (2023), arXiv:2204.03045 [cond-mat.str-el].
- [7] E. Lake, (2018), arXiv:1802.07747 [hep-th].
- [8] X.-G. Wen, *Phys. Rev. B* **99**, 205139 (2019), arXiv:1812.02517 [cond-mat.str-el].
- [9] C. Córdova, T. T. Dumitrescu, and K. Intriligator, *JHEP* **02**, 184 (2019), arXiv:1802.04790 [hep-th].
- [10] Y. Hidaka, Y. Hirono, and R. Yokokura, *Phys. Rev. Lett.* **126**, 071601 (2021), arXiv:2007.15901 [hep-th].
- [11] M. Qi, L. Radzihovsky, and M. Hermele, *Annals Phys.* **424**, 168360 (2021), arXiv:2010.02254 [cond-mat.str-el].
- [12] Y. Hirono, M. You, S. Angus, and G. Y. Cho, *SciPost Phys.* **16**, 050 (2024), arXiv:2207.00854 [cond-mat.str-el].
- [13] R. H. Kraichnan, *J. Fluid Mech.* **47**, 525 (1971).
- [14] R. Fjørtoft, *Tellus* **5**, 225 (1953).
- [15] P. Tabeling, *Phys. Rept.* **362**, 1 (2002).
- [16] A. Alexakis and L. Biferale, *Phys. Rept.* **767–769**, 1 (2018).
- [17] H. K. Moffatt, *J. Fluid Mech.* **35**, 117 (1969).
- [18] L. Biferale, S. Musacchio, and F. Toschi, *Phys. Rev. Lett.* **108**, 164501 (2012).
- [19] N. Sogabe and N. Yamamoto, *Phys. Rev. D* **99**, 125003 (2019), arXiv:1903.02846 [hep-th].
- [20] Y. Hidaka, M. Nitta, and R. Yokokura, *Phys. Lett. B* **808**, 135672 (2020), arXiv:2006.12532 [hep-th].
- [21] Y. Hidaka, M. Nitta, and R. Yokokura, *JHEP* **01**, 173 (2021), arXiv:2009.14368 [hep-th].
- [22] Y. Choi, H. T. Lam, and S.-H. Shao, *JHEP* **09**, 067 (2023), arXiv:2212.04499 [hep-th].
- [23] R. Yokokura, (2022), arXiv:2212.05001 [hep-th].
- [24] N. Yamamoto and R. Yokokura, *JHEP* **07**, 045 (2023), arXiv:2305.01234 [hep-th].
- [25] O. Bergman, N. Jokela, G. Lifshytz, and M. Lippert, *JHEP* **10**, 034 (2011), arXiv:1106.3883 [hep-th].
- [26] H. Ooguri and M. Oshikawa, *Phys. Rev. Lett.* **108**, 161803 (2012), arXiv:1112.1414 [cond-mat.mes-hall].
- [27] N. Yamamoto and R. Yokokura, *Phys. Rev. D* **106**, 105004 (2022), arXiv:2203.02727 [hep-th].
- [28] Y. Choi, H. T. Lam, and S.-H. Shao, *Phys. Rev. Lett.* **129**, 161601 (2022), arXiv:2205.05086 [hep-th].
- [29] C. Cordova and K. Ohmori, *Phys. Rev. X* **13**, 011034 (2023), arXiv:2205.06243 [hep-th].
- [30] M. Joyce and M. E. Shaposhnikov, *Phys. Rev. Lett.* **79**, 1193 (1997), arXiv:astro-ph/9703005.
- [31] Y. Akamatsu and N. Yamamoto, *Phys. Rev. Lett.* **111**, 052002 (2013), arXiv:1302.2125 [nucl-th].

- [32] M. Crossley, P. Glorioso, and H. Liu, *JHEP* **09**, 095 (2017), [arXiv:1511.03646 \[hep-th\]](#).
- [33] H. Liu and P. Glorioso, *PoS TASI2017*, 008 (2018), [arXiv:1805.09331 \[hep-th\]](#).
- [34] Y. Hirono, D. Kharzeev, and Y. Yin, *Phys. Rev.* **D92**, 125031 (2015), [arXiv:1509.07790 \[hep-th\]](#).
- [35] H. Tashiro, T. Vachaspati, and A. Vilenkin, *Phys. Rev. D* **86**, 105033 (2012), [arXiv:1206.5549 \[astro-ph.CO\]](#).
- [36] N. Yamamoto, *Phys. Rev. D* **93**, 125016 (2016), [arXiv:1603.08864 \[hep-th\]](#).
- [37] P. V. Buividovich and M. V. Ulybyshev, *Phys. Rev. D* **94**, 025009 (2016), [arXiv:1509.02076 \[hep-th\]](#).
- [38] M. Mace, N. Mueller, S. Schlichting, and S. Sharma, *Phys. Rev. Lett.* **124**, 191604 (2020), [arXiv:1910.01654 \[hep-ph\]](#).
- [39] M. S. Turner and L. M. Widrow, *Phys. Rev. D* **37**, 2743 (1988).
- [40] B. Ratra, *Astrophys. J. Lett.* **391**, L1 (1992).